Quantitative live cell imaging of glucocorticoid receptor dynamics in the nucleus

Keizer, V.I.P.

4 DIFFERENCES IN GLUCOCORTICOID RECEPTOR AND ESTROGEN RECEPTOR INTRANUCLEAR DISTRIBUTION

Veer I.P. Keizer, Stefano Coppola, Thomas Schmidt, Marcel J.M. Schaaf

ABSTRACT

Although the clustering of transcription factors in nuclear foci in the nucleus is a frequently observed phenomenon, these foci have been described poorly thus far. Here, we have quantitatively characterized foci of the glucocorticoid receptor (GR) and the estrogen receptor (ER). These two transcription factors are closely related members of the nuclear receptor superfamily and are involved in essential processes in all eukaryotes. We compared their distribution and found that the GR clusters in fewer foci that are larger than the foci in which the ER is clustered. In contrast, the intensity of the foci, which corresponds with the number of transcription factors within a focal domain, was similar for both receptors. The ER and GR recognize different DNA binding motifs. We exploited the close homology of the two receptors in their DNA-binding-domain, to create mutants that exchanged recognition of the binding motif. Using these mutants, we found that there is no effect of targeting to specific DNA binding motifs (HRE) on the characteristics of nuclear. Therefore, we suggest that interaction with DNA through the DNA binding domain may be required for the formation of foci, but that the actual formation of receptor-specific foci depends on other receptor domains interacting with nuclear factors causing clustering of the receptor.

4.1 INTRODUCTION

In eukaryotic cells, the nucleus contains the DNA, which is organized by folding into nucleosomes and higher order structures along each chromosome. The nucleus is a highly organized organelle and contains several specific nuclear bodies, of which the nucleolus is the most evident. Proteins that are known to interact with the DNA, such as transcription factors, appear to be organized in a specific manner. Transcription factors function as regulators of gene expression. To this end, they bind to specific DNA target sites and recruit cofactors to activate or repress genes. When studying transcription factors in the nucleus of a cell, either by immunocytochemistry or expression of green fluorescent protein (GFP)-tagged proteins, it has often been noted that their distribution is not homogeneous, but that they are organized in foci within the nucleus. These foci appear to be relevant to transcription as they colocalized active transcription and inhibition of transcription by α-amanitin prevented the formation of dioxin receptor foci (1). In contrast, for another transcription factor, the glucocorticoid receptor (GR) only a partial colocalization with pre-mRNA and RNA polymerase II was found (2,3). For GR it was shown that the existence of these foci depends on DNA binding, dimerization and ligand binding (4–6). Together, these data show that although several determinants of these foci have been identified, the underlying biological mechanism and their exact function is still unclear.

In the present study, we have compared the intranuclear distribution of the GR with that of the estrogen receptor (ER). GR and ER are both steroid receptors, of which the activating ligand is a steroid hormone, and they belong to the superfamily of nuclear receptors. Interestingly, both receptors appear homogenously distributed in the absence of ligand, but form characteristic subdomains upon activation by a ligand. DNA binding of these receptors is mediated through direct interactions with the DNA of amino acids in the proximal box (p-box) of the DNA-binding-domain (DBD). Interestingly, the p-box of the ER differs from the DBD of the GR by only three amino acids, which specify the binding to their DNA target sequences, glucocorticoid-response elements (GREs) or estrogen-response elements (EREs). Previous work has shown that exchanging these three amino acids in

the ER for the corresponding amino acids in the GR, changes the binding preference of the ER to GR DNA targets (7,8). Here we have used the ER and GR as model transcription factors to study the molecular mechanisms underlying the formation of transcription factor foci in the nucleus. We have investigated the intranuclear distribution of ER and GR (GFP-tagged and by immunocytochemistry on endogenous receptors) to see if they have similar distributions in the nucleus. In addition, we have used mutations in the p-box of Gr and ER to change their specific DNA binding preference to see if specific binding to EREs or GREs is related to the appearance of nuclear foci.

Quantification of the nuclear distribution of transcription factors using images taken by fluorescence microscopy as previously been addressed by measuring the coefficient of variation (CV) (5,6). The CV is obtained by drawing the longest straight line through the image of a nucleus and measuring the variation of the fluorescence intensities along that line. When there are many foci, there is a lot of variation on this line and the CV is high. When the distribution of the transcription factor is more homogeneous, the CV value is lower. Using this method, both Schaaf et al. (5) and Presman et al. (6) show this value to be dependent on ligand binding to the GR. Although this method describes inhomogeneity well, it does not allow for the characterization of the foci themselves. Previously, thresholding methods have been utilized, but they did not allow for relevant variation in the expression levels of the protein (3,4). Here we have studied the number of foci, their size and relative fluorescence intensity for ER and GR. We use spinning disk confocal microscopy coupled with an extensive thresholding approach to identify foci. We show that the size number and fluorescence intensity of these subdomains is different for GR and ER. In addition, we have studied whether the effect of specific DNA binding can account for the differences between these receptors by exchanging the p-box between the two receptors. We show that the difference in distribution is not dependent on binding to specific DNA target sites.

4.2 RESULTS

In the present study, we have performed a quantitative study of GR and ER distributions iin the nucleus of live cells and find determinants of

inhomogeneity in their distribution. To this end, U2OS cell were stably transfected with a construct encoding either a GFP-GR or a GFP-ER fusion protein. Single clones were selected for low expression of the protein to avoid overexpression artefacts. Expression levels were comparable to or slightly higher than endogenous expression in different cell lines (supplemental figure 1). A confocal microscopy image of a representative nucleus after activation with the ligand is shown for each of the selected cell lines in figure 1 (A-F).

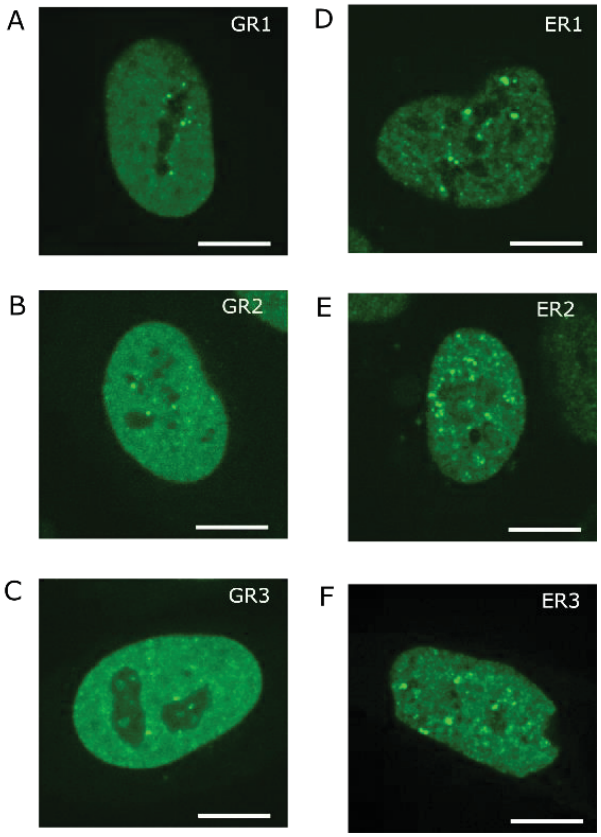

Figure 1. Nuclear distribution of GFP-GR and GFP-ER in U2OS cells (scale bars correspond with 5 µm). A-C. Representative confocal images of U2OS stably expressing GFP-GR clones 1-3. Two hours post activation with ligand (FP, 5 nM). D-F. Representative confocal images of U2OS stably expressing GFP-ER clones 1-3. Two hours post activation with ligand (estradiol, 50 nM).

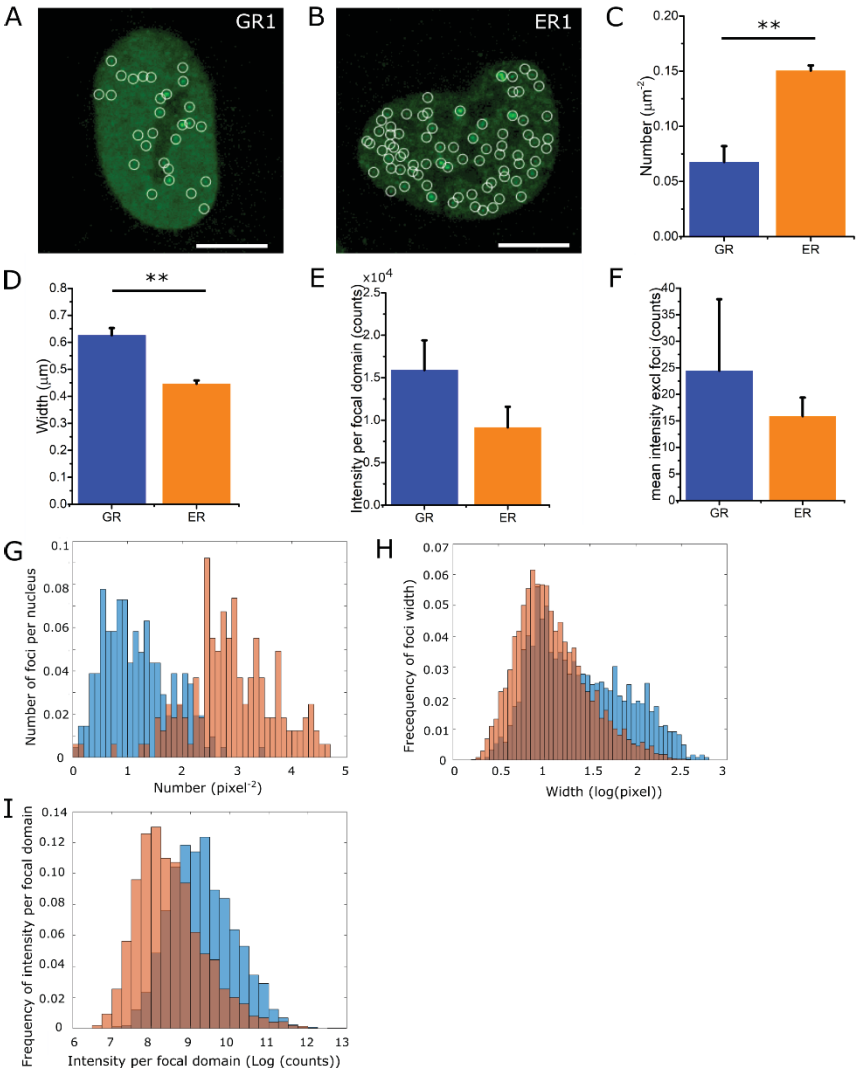

Figure 2. Analysis of GFP-GR and GFP-ER distribution in the nucleus. A-B. Representative confocal image of GFP-GR (A) and GFP-ER (B) distribution in the nucleus. Foci identified after analysis are circled in white (scale bar corresponds with 5 µm). C. Number of GFP-GR and GFP-ER foci per area. D. Width of GFP-GR and GFP-ER foci. E. Integrated intensity per focal domain for GFP-GR and GFP-ER. F. Mean intensity in the nucleus excluding foci for GFP-GR and GFP-ER. G. Histogram of number of foci per nucleus for GFP-GR (blue) and GFP-ER (orange) expressing cells. H. Histogram showing the distribution of the width of GFP-GR (blue) and GFP-ER foci (orange). I. Histogram showing the distribution of integrated intensity per focal domain of GFP-GR (blue) and GFP-ER foci (orange). N=3. Statistical significance tested by two sample t-test. ** refers to a p-value <0.01.

To characterize the nuclear distribution of both receptors in these images, an algorithm for the identification of areas with an increased concentration of receptors ('foci') was developed. In brief, after identification of the individual nuclear area through a customized watershedding procedure, a triangular thresholding was applied. A 3D Gaussian curve was then fitted in areas that remained after thresholding. This procedure was carried out for all cell lines. As an example, an image showing the foci that were identified in a cell expressing GFP-GR and GFP-ER is shown in figure 2 (A and B respectively). In U2OS cells stably expressing GFP-GR at a low expression level (GR1), the number of foci was 0.065 μm^{-2} ± 0.011 μm^{-2}. Given the average surface area a U2OS nucleus at the center of (289 μm^2 (9)), this is equivalent to an average of ~19 foci in one of our confocal microscopy images of a nucleus. In cells expressing GFP-ER (ER1), the number of foci per nuclear area was significantly higher (figure 2C). With 0.16 foci μm^{-2}, a cell expressing GFP-ER showed on average ~46 foci. In addition, the width of the foci was determined. In cells expressing GFP-GR the average width of the foci was 0.60 µm ± 0.023 µm (figure 2D). The width of the foci was found to be significantly smaller in cells expressing GFP-ER: 0.47 µm ± 0.018 µm. The integrated fluorescence intensity of the foci was not significantly different between foci in the GFP-ER and GFP-GR expressing cells (figure 2E). In addition, there was no significant difference in the average fluorescence intensity measured outside the foci (figure 2F). Subsequently, we made histograms for both GR and ER showing the distribution of the number of foci per cell, the distribution of the width and the integrated intensity of the individual focal domains. All histograms showed a unimodal distribution. This reveals that within the cell population there are no subpopulations of cells with different characteristics and that only one population of foci can be distinguished within these cells (figure 2G-I).

The different clonal cell lines generated for each receptor (GR1, GR2, GR3 and ER1, ER2 and ER3) showed differences in the expression level of GFP-GR or GFP-ER (supplemental figure 2A). However, there was no difference in the number of foci or the width of the foci between the cell lines expressing GFP-GR (supplemental figure 2B-C). This was also true for the cell lines expressing

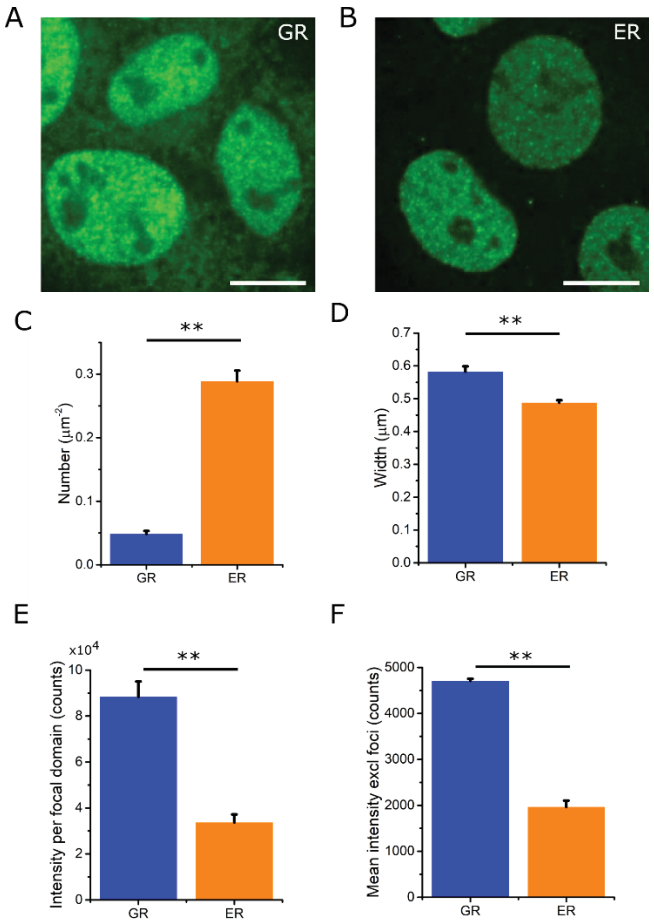

Figure 3. Characterization of endogenous glucocorticoid receptor and estrogen receptor foci in MCF7 cells. A-B. Representative confocal image of GR (A) and ER (B) distribution in the nucleus (scale bars correspond with 5 µm). Immunostaining was performed using antibodies against the relevant receptor. C. Number of GR and ER foci per area. D. Width of GR and ER foci. E. Integrated intensity per focal domain for GR and ER. F Mean intensity in the nucleus excluding foci for GR and ER. N=3. Statistical significance tested by two sample t-test. ** refers to a p-value <0.01.

GFP-ER, and it indicates that these parameters are independent of the expression levels of the receptors. Differences were found in the intensity per focal domain and the mean intensity outside the foci (supplemental figure 2D-E) which demonstrates that these parameters are dependent on the expression level of the receptors.

One GR (GR1) and one ER (ER1) cell line were chosen to study the effect of the expression level in more detail. The number of foci, their width and integrated intensity were plotted against the mean fluorescence intensity of the nucleus in which the focal domain was detected. For GFP-GR the number and width of the foci did not correlate with the mean intensity of the nucleus, verifying that these parameters were not affected by the expression level (supplemental figure 3A-B). For GFP-ER foci the width, but not the number of foci was correlated with the mean intensity of the nucleus (supplemental figure 3E-F). For both GFP-GR and GFP-ER the intensity per focal domain correlated with the mean intensity of the nucleus (supplemental figure 3C,G). This is expected as the focal domains contribute to the mean intensity of the nucleus. For GFP-GR and GFP-ER foci, the mean intensity outside the foci did not correlate with the mean intensity of nucleus (supplemental figure 3D-H), indicating that the intensity inside the focal domains was the biggest contributor to the mean intensity of the nucleus. The intensity per focal domain did not correlate with the mean intensity outside the nucleus (data not shown).

To investigate possible effects of the imaging procedure, the exposure time was varied between 10 and 100 milliseconds and the effect on the different parameters was determined. The mean intensity increased with increasing exposure time (supplemental figure 4A). The exposure time had no effect on the number of foci of either GFP-GR or GFP-ER (supplemental figure 4B), but there was an effect of exposure time on the width of GFP-ER foci and not the GFP-GR foci (figure 4C). The mean intensity inside the foci increased as the exposure time was increased for GFP-GR and GFP-ER foci, but this effect was not significant for GFP-GR (supplemental figure 4D). The intensity outside the focal domain also increased with increasing exposure time for GFP-ER foci, but this effect was not significant for GFP-ER foci (supplemental figure 4E).

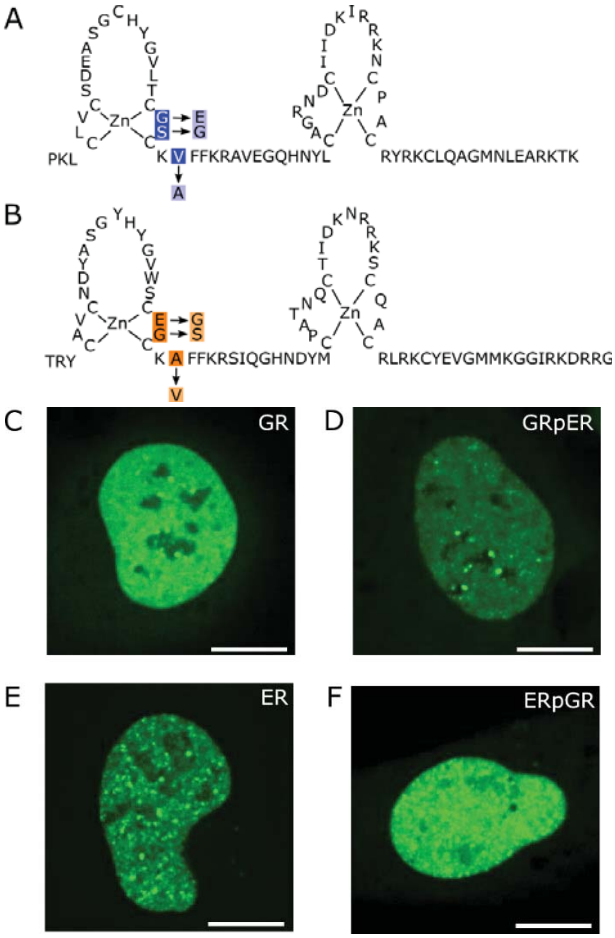

Figure 4. Analysis of WT and mutant steroid receptor distribution in the nucleus (scale bars correspond with 5 µm). A. Amino acid sequence of the GR DNA-binding-domain. The amino acids indicated in dark blue were mutated to the amino acids indicated in light blue to obtain a GR with the p-box of the ER (GRpER). B. Amino acid sequence of the ER DNA-binding-domain. The amino acids indicated in dark orange were mutated to the amino acids indicated in light orange to obtain a ER with the p-box of the GR (ERpGR). C. Representative confocal image of U2OS transiently expressing GFP-GR. Distribution of the receptor in the nucleus two hours post activation with the ligand (FP, 5 nM). D. Representative confocal image of U2OS transiently expressing GFP-GRpER. Distribution of the receptor in the nucleus two hours post activation with ligand (FP, 5 nM). E. Representative confocal image of U2OS transiently expressing GFP-ER. Distribution of the receptor in the nucleus two hours post activation with ligand (estradiol, 50 nM). F. Representative confocal image of U2OS transiently expressing GFP-ERpGR. Distribution of the receptor in the nucleus after activation with ligand (estradiol, 50 nM).

Next, we studied the distribution of endogenously expressed GR and ER. Since this requires immunostaining of fixed cells, we first investigated the effect of fixation. For this purpose, stably transfected U2OS cells were imaged prior to fixation and 30 minutes after fixation. For this purpose, MCF7 cells were fixed after activation of the receptor with the appropriate ligand, and an immunostaining was performed for either the GR or the ER. A representative confocal image of GR and ER distribution in the nucleus is shown in figure 3A and 3B respectively. The differences between ER and GR distribution as observed in U2OS cells for the number and width of the foci were also observed for the endogenous receptors in the MCF7 cells (figure 3C-D). Opposite to the results in U2OS cells, the integrated focal domain intensity and mean intensity outside the foci were higher for the GR than for the ER (figure 3E-F). Since we showed that these parameters correlate with the expression level, this is most likely due to higher expression levels. Alternatively, the efficiency of the immunostaining could be different between the GR and ER immunocytochemistry.

Subsequently, we have investigated the effect of specific DNA binding on the nuclear distribution of ER and GR. In figure 4A, a schematic of the DBD of GR is given including the three amino acids in the p-box that specify the binding of the receptor to a GRE or an ERE (indicated in dark blue). We have mutated these amino acids in the GR to correspond to those in the ER (light blue). In this manner a GR with the p-box of the ER was created, which hereafter is termed GRpER. The reciprocal, the ER with a p-box that corresponds with a GR was also constructed (ERpGR, figure 4B).

These constructs or the wildtype (WT) receptor were transiently transfected into U2OS cells. Activation of the receptor was carried out using the ligand recognized by the original receptor. Representative confocal images of cells expressing these receptors are shown in figure 4C-F. As observed previously in the stable cell lines, the wild type GFP-ER foci were significantly more numerous than the GFP-GR foci (figure 5A). However, there was no significant difference between GFP-GR and GFP-GRpER or between GFP-ER and GFP-ERpGR.

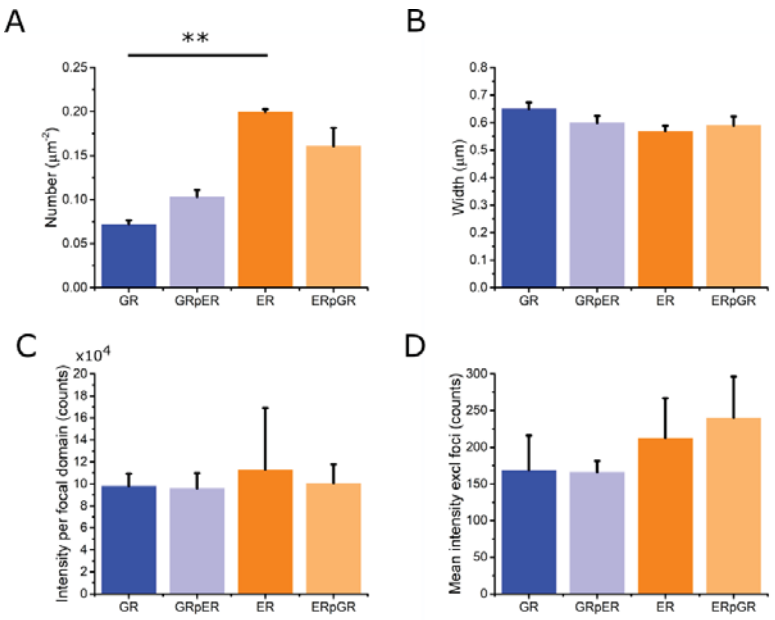

Figure 5. Analysis of WT and mutant steroid receptor distribution in the nucleus. A. Number of GFP-GR and GFP-ER foci (WT or mutated) per area. B. Width of GFP-GR and GFP-ER foci (WT or mutated). C. Integrated per focal domain for GFP-GR and GFP-ER (WT or mutated). D. Mean intensity in the nucleus excluding foci for GFP-GR and GFP-ER (WT or mutated). F. Total intensity in foci normalized for the mean intensity of the nucleus for GFP-GR and GFP-ER (WT or mutated). G. Mean intensity per nucleus for GFP-GR and GFP-ER expressing cells. N=3. Statistical significance tested by two sample t-test. ** refers to a p-value <0.01.

The significant difference between the width of the GFP-GR and GFP-ER foci, observed using the stable U2OS cell lines, was lost in this experiment in which transient transfections were used (figure 5B). There was no significant difference between the GFP-GR and GFP-GRpER or the GFP-ER and GFP-ERpGR when their width, integrated intensity per focal domain, or the mean intensity outside the foci was analyzed (figure 5C-D). These data indicate that specific DNA binding, driven by the p-box in the DBD, does not determine the formation of foci in the nucleus.

4.3 Discussion

In this study, we have quantified the distribution of the ER and GR into focal domains inside the nucleus. Our data show that GR is localized in a smaller number of foci with a larger width. GR and ER foci contain a similar number of receptors. When expression levels increase, more receptors reside in the foci, but their size and number remains unchanged. The foci do not represent specific DNA binding.

The nuclear distribution of a fluorescently tagged GR and ER was measured in stably transfected U2OS cell lines. Stable cell lines with low expression, comparable to endogenous GR expression were selected. The number of foci for the ER was significantly higher than for the GR and the width of the ER foci was significantly smaller. In contrast, the total fluorescence intensity of each focal domain was not significantly different between ER and GR foci. This indicates that although the average size of the GR focal domain is bigger, there are not significantly more receptors present than in an ER focal domain. In addition, the fluorescence intensity in the nucleus outside the foci was comparable for both receptors, indicating that the number of molecules outside foci is similar for ER and GR and that the fraction of receptors that is present inside the foci is larger for ER. Therefore, we can conclude that ER is present in the nucleus in more foci than the GR and that these foci are smaller than the ER foci. Differences between two related receptors were previously also observed for another transcription factor sp1 and sp3 (10).

Several control experiments were performed to ensure the validity of the parameters we determined to describe the foci. In the experiments in which we varied the exposure time, we found that the exposure time did not correlate with the number or width of the foci for GFP-GR. For GFP-ER foci we found an effect on the number of foci. The exposure time did correlate positively with the intensity inside the focal domains. In experiments in which we studied the effect of the expression level, we found that there was no correlation between the mean fluorescence intensity of the nucleus (which is a measure for the expression level), and the number of foci or their width. Thus, with increasing expression levels no new foci appeared that previously remained undetected. However, the average fluorescence intensity of the

foci increased with increasing expression levels. This indicates that the foci contain more molecules but do not cover a larger area when more receptors are available in the nucleus. Apparently, within a restricted number of areas within the nucleus that cover a limited size, there is a seemingly unlimited number of docking sites for ER and GR.

By exchanging the three amino acids that specify binding to GREs or EREs, the GRpER mutant and ERpGR mutant were created. Interestingly, no significant effect was observed between the mutants and their original WT receptor. This strongly suggests that the distribution of receptors into nuclear foci does not directly represent binding to specific DNA binding sites. However, it was previously shown that organization of the GR into foci is dependent on the presence of a functional DBD (5). It is possible that DNA binding is a prerequisite for the formation of foci, but that the N-terminal-domain or ligand-binding-domain mediate crucial interactions with other factors that instigate the formation of foci, of which the size and number differs between receptors. Alternatively, these foci represent receptor specific degradation sites. It has been shown that the glucocorticoid receptor interacting protein 1 colocalizes with a subunit of the proteasome in discrete nuclear foci (11). Interestingly, it has also been shown that subunits of the proteasome colocalize with the receptor at the DNA and possibly assist dissociation of the receptor from the DNA (12).

In conclusion, there are large differences between ER and GR foci inside the nucleus, which are not a result of binding to different DNA target sites. Although DNA binding may be required for the formation of foci, we suggest that other factors interacting in a receptor-specific manner with domains outside the DBD determine the number and size of steroid receptor foci in the nucleus.

4.4 Material and Methods

DNA plasmids

The pEGFP-GR and pmCherry-GR plasmid were constructed by exchanging the EYFP coding sequence in the original pEYFP-GR-C1 plasmid for a EGFP or mCherry sequence using NheI and BsrGI restriction sites (original pEYFP-GR plasmid described in (13)). A pEGFP-ER plasmid with the exact same linker sequence between the GFP and ER as between the GFP and GR in pEGFP-GR was constructed through PCR of the human ERalpha coding sequence using primers containing XhoI and BamHI restriction sites. A pmCherry-ER plasmid was constructed by exchanging the EGFP sequence in the pEGFP-ER plasmid for a mCherry using the NheI and XhoI sites. The pEGFP-GRpER and the pEGFP-ERpGR plasmid were generated by site-directed mutagenesis using the QuikChange II Site-Directed Mutagenesis Kit (Agilent, Santa Clara, CA). Successful mutation was confirmed by sequence analysis.

Cell culture and generation of stable cell lines

U2OS and A549 cells were cultured in Dulbecco's Modified Eagle's Medium (DMEM, ThermoFisher Scientific, Waltman, MA) without phenol red supplemented with 10% fetal calf serum (FCS) at 37°C with 5% CO_2. Transfection was carried out using polyethylenimine (PEI) at a 3:1 ratio PEI to DNA. DNA and PEI were diluted separately in media without FCS. The PEI mixture was added to the DNA mixture and vortexed briefly. This mix was incubated at room temperature for 20 minutes. Medium was refreshed the following day. For the generation of stable cell lines, transfection was carried out using at least $1x10^6$ cells. After one day selection medium containing 700 µg/ml G418 was applied to the cells. After approximately ten days cells were seeded thinly in a 100 mm petri dish. Single clones were selected and transferred to a 12 well plate.

Western blot

Cells were induced with the relevant ligand for two hours and samples were extracted on ice using RIPA buffer. After collection of the cells by scraping, the sample was sonicated and centrifuged. The supernatant was transferred to a new tube. Laemli buffer was added and the sample was incubated for 10 minutes at 95°C. The sample was run on a 4-15% gradient precast gel (Bio-

Rad, Veenendaal, Netherlands). The gproteins were blotted onto a nitrocellulose membrane using the turbo transfer system (Bio-Rad, Veenendaal, Netherlands). Blocking was performed for one hour using 5% milk powder in PBS-Tween. A primary rabbit antibody against the GR and a primary rabbit antibody against actin were incubated overnight (1:500 and 1:1000 respectively, Abcam, Cambridge, UK). A secondary peroxidase-conjugated anti-rabbit antibody was used in combination with the Clarity Western ECL blotting substrate to visualize the protein band (Bio-Rad, Veenendaal, Netherlands). Quantification was performed using ImageJ by calculating the integrated intensity within a predetermined region around all bands.

SPINNING DISC CONFOCAL MICROSCOPY

One day prior to transfection, cells were plated in 6-well plates (Sarstedt, Etten-Leur, Netherlands), containing coverglasses (ThermoFisher Scientific, Waltman, MA). One day after transfection, cells were induced with the relevant ligand (5 nM fluticasone proprionate (FP, Sigma Aldrich, Zwijndrecht, The Netherlands) or 50 nM estradiol (Sigma Aldrich, Zwijndrecht, The Netherlands)). Three to six hours after addition of the ligand, the coverglass on which the cells had been plated was placed in a metal ring holder and 1 ml Fluobrite medium (ThermoFisher Scientific, Waltman, MA) was added. Cells were imaged at 37°C and 5% CO_2 using a spinning disk confocal microscope equipped with a 100x/1.4 NA oil-immersion objective (Carl Zeiss, Breda, Netherlands). For cells expressing GFP conjugated constructs, illumination was performed using a 488 nm argon laser at an intensity of 2.5 kW/cm^2. For cells expressing mCherry conjugated constructs, illumination was performed using a 561 nm argon laser at an intensity of 2.5 kW/cm^2. Illumination of the sample for 50 ms was controlled through an acousto-optical tunable filter (AA Opto Electronic, Orsay, France). Images were recorded on a back-illuminated CCD camera (Princeton, Instruments, Trenton, NJ) with 0.138 µm/pixel. Three individual experiments were performed in which at least each 30 cells were imaged per condition.

IMAGE ANALYSIS

To identify foci and quantify their characteristics Matlab (Mathworks, Eindhoven, the Netherlands) was utilized and a script was developed. The nucleus of each cell was identified automatically using marker-controlled watershed segmentation. In brief, foreground objects were marked through opening-by-reconstruction and closing-by-reconstruction. Regional maxima were identified and subsequently the edges were cleaned. Regions with an area smaller than 3000 pixels were excluded to avoid inclusion of artefacts present in the image. The area of each nucleus was measured and stored separately as a mask. This mask was applied to the original image. Subsequently, possible positions of individual foci were obtained by thresholding the grey scale image using the triangle method (14). This allowed for thresholding that takes into account the fluorescence intensities outside the foci since these can differ within an image and across images. At the identified positions, a Gaussian was fitted to the original image. The fitted foci were removed from the image and the process was iterated to identify foci in close proximity of each other. Foci with a relative fitting error larger than 0.3 were discarded.

REFERENCES

1. Elbi C, Misteli T, Hager GL. Recruitment of dioxin receptor to active transcription sites. Mol Biol Cell. 2002;

2. van Steensel B, Jenster G, Damm K, Brinkmann AO, van Driel R. Domains of the human androgen receptor and glucocorticoid receptor involved in binding to the nuclear matrix. J Cell Biochem. 1995;

3. van Steensel B, Brink M, van der Meulen K, van Binnendijk EP, Wansink DG, de Jong L, et al. Localization of the glucocorticoid receptor in discrete clusters in the cell nucleus. J Cell Sci. 1995;

4. Stortz M, Presman DM, Bruno L, Annibale P, Dansey M V., Burton G, et al. Mapping the Dynamics of the Glucocorticoid Receptor within the Nuclear Landscape. Sci Rep. 2017;

5. Schaaf MJ, Lewis-Tuffin LJ, Cidlowski JA. Ligand-selective targeting of the glucocorticoid receptor to nuclear subdomains is associated with decreased receptor mobility. Mol Endocrinol. 2005;19(6):1501–15.

6. Presman DM, Alvarez LD, Levi V, Eduardo S, Digman MA, Martí MA, et al. Insights on glucocorticoid receptor activity modulation through the binding of rigid steroids. PLoS One. 2010;

7. Voss TC, Schiltz RL, Sung MH, Yen PM, Stamatoyannopoulos JA, Biddie SC, et al. Dynamic exchange at regulatory elements during chromatin remodeling underlies assisted loading mechanism. Cell. 2011;

8. Mader S, Kumar V, De Verneuil H, Chambon P. Three amino acids of the oestrogen receptor are essential to its ability to distinguish an oestrogen from a glucocorticoid-responsive element. Nature. 1989;

9. Koch B, Sanchez S, Schmidt CK, Swiersy A, Jackson SP, Schmidt OG. Confinement and Deformation of Single Cells and Their Nuclei Inside Size-Adapted Microtubes. Adv Healthc Mater. 2014;

10. He S, Sun J-M, Li L, Davie JR. Differential Intranuclear Organization of Transcription Factors SP1 and SP3. Mol Biol Cell. 2005;

11. Baumann CT, Ma H, Wolford R, Reyes JC, Maruvada P, Lim C, et al. The glucocorticoid receptor interacting protein 1 (GRIP1) localizes in discrete nuclear foci that associate with ND10 bodies and are enriched in components of the 26S proteasome. Mol Endocrinol. 2001;

12. Stavreva DA, Muller WG, Hager GL, Smith CL, McNally JG. Rapid glucocorticoid receptor exchange at a promoter is coupled to transcription and regulated by chaperones and proteasomes. Mol Cell Biol. 2004;24(7):2682–97.

13. Schaaf MJ, Cidlowski JA. Molecular determinants of glucocorticoid receptor mobility

in living cells: the importance of ligand affinity. Mol Cell Biol. 2003;23(6):1922–34.

14. Zack GW, Rogers WE, Latt SA. Automatic measurement of sister chromatid exchange frequency. J Histochem Cytochem. 1977;

4.5 SUPPLEMENTAL FIGURES

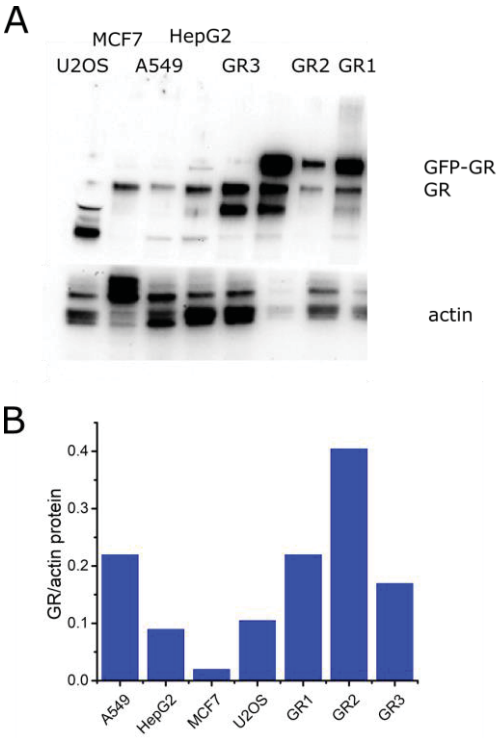

Supplemental figure 1. Expression of endogenous GR and stable expression of GFP-GR in different cell lines. Cells were immunostained using an antibody against the GR. Quantification of western blot results through optical density measurement of protein bands in the blot and normalization to actin. GR1-3 correspond with the three cell lines that stably express GFP-GR.

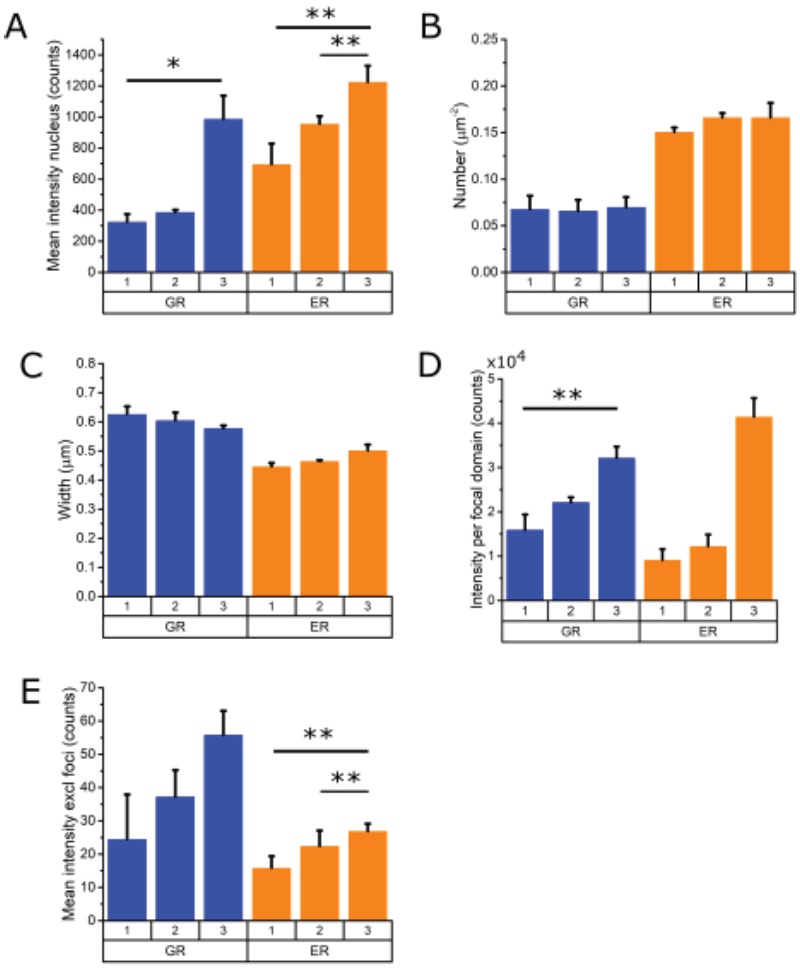

Supplemental figure 2. Homogeneity amongst single clone cell lines. A. Mean intensity per nucleus of U2OS cells expressing GFP-GR or GFP-ER in three single clone cell lines. B. Number of GFP-GR and GFP-ER foci per area in three different single clone cell lines. C. Width of GFP-GR and GFP-ER foci in three different single clone cell lines. D. Integrated intensity per focal domain of GFP-GR and GFP-ER foci in three different single clone cell lines. E. Mean intensity in the nucleus excluding GFP-GR and GFP-ER foci for three different single clone cell lines.

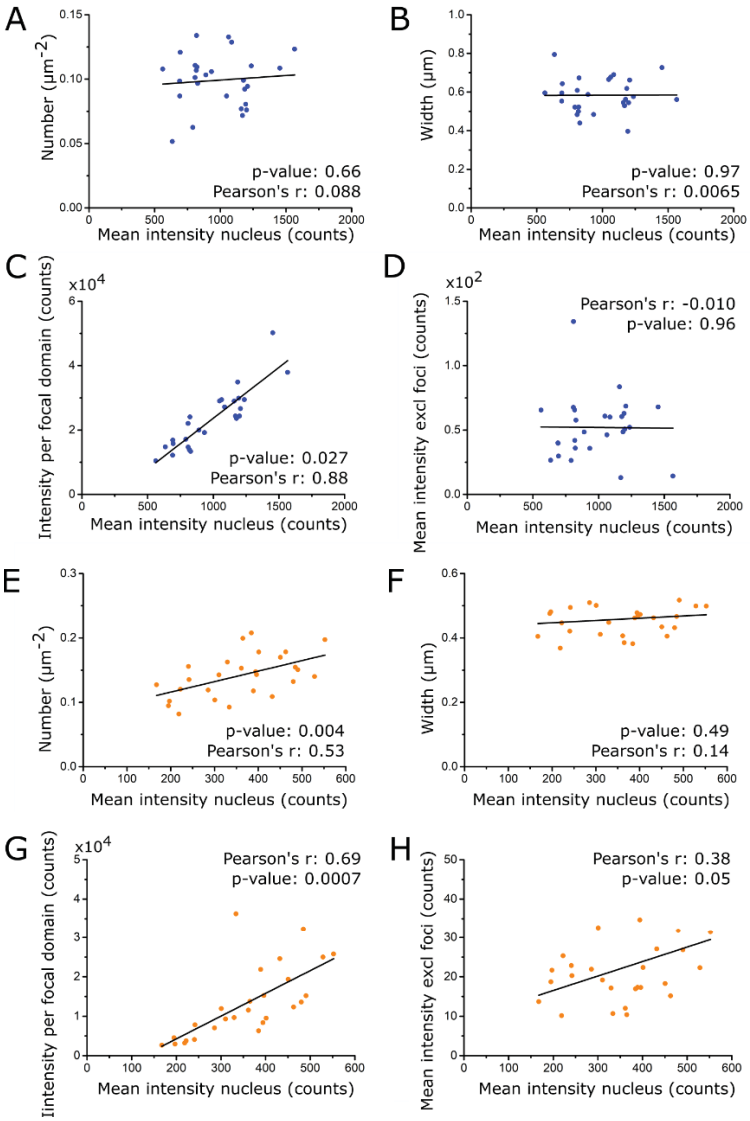

Supplemental figure 3. The effect of expression levels on different parameters. Pearson's correlation coefficient is given as a measure of correlation between the mean intensity per nucleus excluding foci and the specific parameter. No correlation was significant based on regression analysis. A. The effect of the mean intensity per nucleus excluding foci on the number of GFP-GR foci identified per area. B. The effect of the mean intensity per nucleus excluding foci on the width of GFP-GR foci. C. The effect of the mean intensity per nucleus excluding foci on integrated intensity per focal domain for GFP-GR foci. D. The effect of the mean intensity per nucleus excluding foci on the number of GFP-ER foci identified per area. E.

The effect of the mean intensity per nucleus on the width of GFP-ER foci. F. The effect of the mean intensity per nucleus excluding foci on integrated intensity per focal domain of GFP-ER foci.

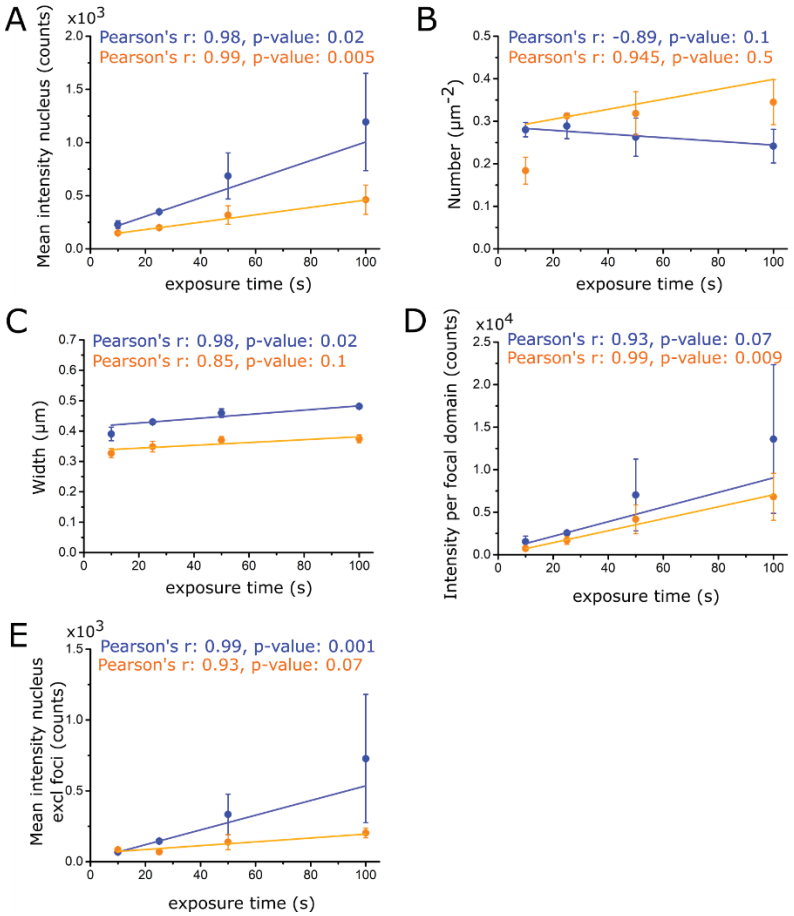

Supplemental figure 4. The effect of exposure time on different parameters for GFP-GR (blue) and GFP-ER (orange) foci. Exposure times of 10, 25, 50 and 100 ms were used. Pearson's correlation coefficient is given as a measure of correlation between the mean intensity per nucleus excluding foci and the specific parameter. N=3. Significance was calculated based on regression analysis (p-value). A. The effect of exposure time on the GFP-GR or GFP-ER foci intensity normalized for the mean intensity of the nucleus. B. The effect of exposure time on the mean intensity in the nucleus of cells expressing GFP-GR or GFP-ER. B. The effect of exposure time on the number of GFP-GR and GFP-ER foci per area. C. The effect of exposure time on the width of GFP-GR and GFP-ER foci. D. The effect of exposure time on integrated intensity per focal domain of GFP-GR and GFP-ER foci. E. The effect of exposure time on the mean intensity excluding GFP-GR or GFP-ER foci.